Persistence of Well-Defined Collective Excitations in a Molten Transition Metal

F. J. Bermejo,[1] M. L. Saboungi,[2] D. L. Price,[2] M. Alvarez,[1] B. Roessli,[3] C. Cabrillo,[1] and A. Ivanov[4]

[1]*Consejo Superior de Investigaciones Científicas, Serrano 119-123, E-28006 Madrid, Spain*

[2]*Argonne National Laboratory, Argonne, Illinois 60439*

[3]*Laboratory for Neutron Scattering, ETH Zurich & Paul Scherrer Institut, CH-5232 Villigen PSI, Switzerland*

[4]*Institut Laue Langevin, BP156, F-38042 Grenoble, Cedex 9, France*

(Received 25 January 2000)

Well-defined microscopic collective excitations are found in liquid Ni at 1763 K by means of inelastic neutron scattering. Such excitations are supported by the liquid despite an anharmonic character of its thermodynamic functions. Consideration of the detailed shape of the interionic pair potential provides a way to understand why atomic motions at microscopic scales behave in a way much closer to the alkali metals than to the liquefied rare gases.

PACS numbers: 61.25.Mv, 61.12.–q, 62.30.+d

Our present picture of collective atomic motions in classical monatomic liquids portrays them in terms of a few discrete eigenmodes of a fluid continuum. This mesoscopic description, valid within the thermodynamic limit, encompasses the relevant dynamics within a wave-vector-dependent frequency spectrum $S(Q, \omega)$ known as the Rayleigh-Brillouin triplet. It reproduces the shape of the experimental spectrum at scales larger than few hundreds of Å [1], where the microscopic details are of scant importance. Beyond such limit and up to length scales comparable to $2\pi/Q_p$ where the static structure factor $S(Q)$ shows its maximum, the excitation spectrum measurable by radiation scattering experiments may show well-defined peaks at finite frequencies which cannot be realistically identified with hydrodynamic sound, but should rather be viewed as microscopic motions paralleling phonon excitations in a crystal. These motions were understood [2,3] in terms of a simple model which predicts the occurrence of independent density oscillations with frequency $\omega_Q = \frac{Q^2 k_B T}{MS(Q)}$ [4], with M being the particle mass, having a lifetime long enough to appear as well-resolved peaks in $S(Q, \omega)$. Such a view, which is borne out by data on molten alkali and some heavier sp metals [3,5], has a thermodynamic consequence which implies that the ratio of specific heats at melting $\gamma = C_p/C_v \approx 1$ and that $C_p/Nk_B \approx 3R$, that is, the liquid is thought of as a collection of harmonic, Einstein oscillators. In contrast, liquefied rare gases support well-defined excitations at wave vectors not far beyond those signaling the crossover from hydrodynamics to the microscopic regime [1]. Such disparate behavior leads to the consideration of the "harmonic-liquid" character as a prerequisite for a liquid to support these kind of excitations. This was further quantified in terms of a criterion based on the curvature about the main minimum of the pair potential [6]. Other liquid metals and semimetals explored so far [7] show, however, that the condition of having a marked harmonic character in the thermodynamic functions is not sufficiently strong to enable the liquid to propagate an excitation of short wavelength. Furthermore, some fairly anharmonic liquids such as *para*-H_2 [7] have been shown to sustain the modes referred to, due to large quantum effects arising from their low mass and the low temperatures close to their triple point.

Liquid Ni constitutes an optimum benchmark to clarify the extent of validity of the picture drawn above. At melting ($T_m = 1728.15$ K) its specific heat $C_p/Nk_B = 4.6R$ is well above the harmonic value ($3R$) and $\gamma = 1.88$ is halfway between that of 2.2 of Ar and that of 1.2 of Rb. The differences in thermal and electronic properties of these two metals are thought to arise from the presence of $3d$ electrons in Ni. These, however, show a scant effect on the microscopic liquid structure which looks rather similar to those of the liquid alkali metals once the different sizes of the electron cores are accounted for. The transport and kinetic properties are, however, far more sensitive to electronic structure details. In particular, the shear viscosity of liquid Ni at melting reaches 5.64 mPa s, and the apparent activation energy for viscous flow amounts to $\approx$29 J mol^{-1} while the alkali metals (from Na to Cs) have viscosities of about 0.50–0.70 mPa s and activation energies $\approx$5 J mol^{-1} [8]. If compared with the well-studied case of liquid Pb, one again obtains figures of 2.6 mPa s and $\approx$8 J mol^{-1}, respectively. The values just quoted indicate that such differences are not due to the disparate atomic masses and melting temperatures of the liquids being compared but should rather be attributed to peculiarities of the interionic potentials. On such a basis, one would expect that only overdamped modes would be supported by the liquid close to melting since their lifetimes would be severely shortened by viscous damping. However, as illustrated here, the presence of relatively well-defined excitations in liquid Ni reveals that the shapes of the interionic potentials need to be considered in greater detail than that of [6] if one wishes to relate them with microscopic dynamic phenomena.

Our interest in studying this liquid was fostered by reports on the highly anomalous behavior of alloys of geophysical interest (Fe-Ni-S) [9] as well as by the availability of simulation results [10] employing realistic

 0031-9007/00/85(1)/106(4)$15.00

potentials and the existence of indirect experimental indications of the presence within the liquid of well-defined excitations [11]. As regards the simulations, well-resolved peaks are seen in $S(Q, \omega)$ persisting up to $Q \approx 1.8$ Å^{-1}, well above $Q_p/2 = 1.54$ Å^{-1}, indicative of an excitation propagating with an adiabatic speed $c_s = 4280$ m s^{-1}.

The measurements were carried out using the IN1 hot-neutron spectrometer located at the Institut Laue Langevin, Grenoble. The sample holder was built from 15 alumina tubes of 78 mm length and 2 mm i.d. filled with Ni wire which were held by two disk flanges of 4 cm diameter on both ends and placed normal to the neutron beam on a circular arrangement of 3 cm diameter. The sample thickness was chosen as a compromise between multiple scattering and inelastic signal-to-noise ratio. The former was estimated to be somewhat below 20% and its main contribution is concentrated at energies below 15 meV. The temperature was set to 1763 K. A representative sample of spectra actually measured using a final wave vector of 8.2 Å^{-1} is shown in Fig. 1. The achieved resolution at the elastic peak was ≈4.5 meV. The usable range of momentum transfers was bound within $0.8 \leq Q \leq 3.5$ Å^{-1}. The measured spectra for Q values beyond 1.5 Å^{-1} show a contribution arising from the high-energy phonons of the alumina container. Fortunately, this was easy to identify since it gives rise to a very strong peak at about 52 meV [12], the intensity of which is modulated by the alumina powder diffraction pattern and was easily separated from the response of the liquid metal which appears at considerably lower frequencies. From the spectra displayed in Fig. 1 it is seen that clear inelastic shoulders appear at wave vectors as large as 1.7 Å^{-1}. Their amplitudes with respect to the whole signal vary among some 17% for $Q = 0.8$ Å^{-1}, 30% for $Q = 1.5$ Å^{-1}, and 38% for $Q = 3.5$ Å^{-1}, which are close to the first minimum in $S(Q)$.

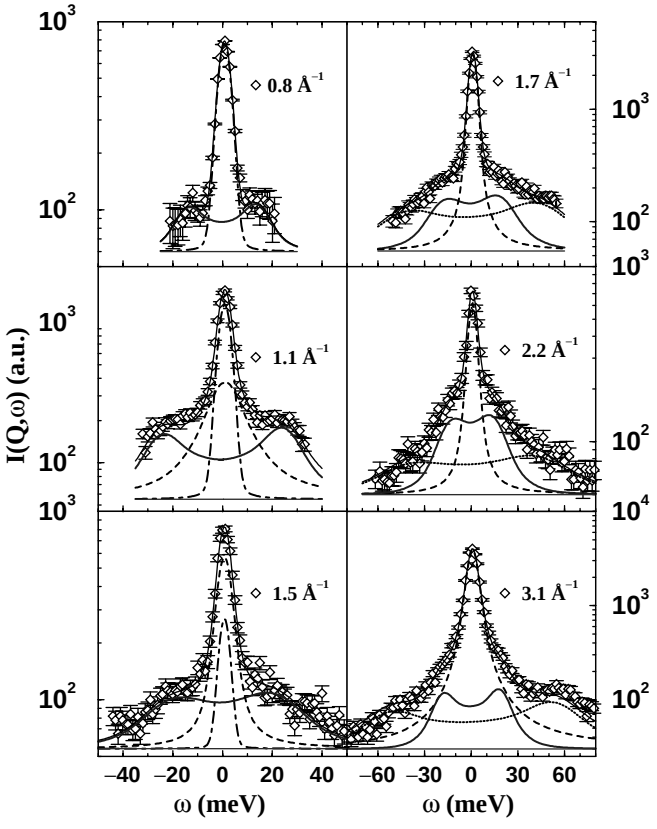

FIG. 1. Spectra as measured on IN1. The graph shows spectra measured at momentum transfers given in the panels. Symbols represent experimental data and lines represent the fitted model functions. Thick solid lines depict the inelastic intensity (DHO), dashed and dashed-dotted lines show the quasielastic components of the coherent and incoherent origins, respectively, and the dotted line in the large-Q spectra shows the intensity arising from the alumina container.

To analyze the spectra in more detail a model function $I_{\mathrm{mod}}(Q, \omega) = AI(Q, \omega) \otimes R(Q, \omega)$ is used, where A stands for a global scaling constant and $R(Q, \omega)$ is the instrumental resolution. Since the ratio of incoherent and coherent neutron cross sections of natural abundance Ni is $\sigma_{\mathrm{inc}}/\sigma_{\mathrm{coh}} \approx 0.3$, both contributions were necessary to account for the quasielastic intensity. The final ingredients of the model function were, therefore,

$$I(Q, \omega) = \frac{\sigma_{\mathrm{coh}}}{\sigma_t} [I_{\mathrm{c.qel}}(Q, \omega) + I_{\mathrm{inel}}(Q, \omega)] + \frac{\sigma_{\mathrm{inc}}}{\sigma_t} I_{\mathrm{i.qel}}(Q, \omega) .$$

The quasielastic contributions $I_{(\mathrm{c,i})\mathrm{qel}}(Q, \omega)$ were represented by two Lorentzians while a damped harmonic oscillator (DHO) was used for $I_{\mathrm{inel}}(Q, \omega)$ [13]. An additional DHO was needed to account for the alumina phonons as shown in some spectra in Fig. 1. The parameters describing the collective dynamics are thus the excitation frequencies Ω_Q, damping terms Γ_Q, and their amplitudes. Within those describing the quasielastic spectrum, only the coherent quasielastic linewidth $\Delta\omega_{\mathrm{qel}}^{\mathrm{coh}}$ and intensity could safely be isolated from the measured intensities, since the incoherent quasielastic component was significantly narrower than the instrument resolution. The measured values for $\Delta\omega_{\mathrm{qel}}^{\mathrm{coh}}$ were within ≈3–14 meV for the explored range of wave vectors.

The Q dependence of the parameters describing the inelastic signal is shown in Fig. 2. Linear hydrodynamic sound is expected to follow a law [6] $\Omega_Q = c_T Q$ with $c_T = c_s/\sqrt{\gamma} = 19.82$ meV Å, that is, the isothermal sound velocity which is given in terms of the adiabatic value and the ratio of specific heats. The data shown in Fig. 2a suggest that such a regime is approached only at the lowest accessible momentum transfer (0.8 Å^{-1}). The lowest data points for Γ_Q shown in Fig. 2b are well approximated by a quadratic function $\Gamma_Q = DQ^2$ with a damping coefficient $D \approx 15$ meV Å^2. The highest frequencies shown in Fig. 2a are ≈15% smaller than the highest phonon frequencies of the crystalline solid [14].

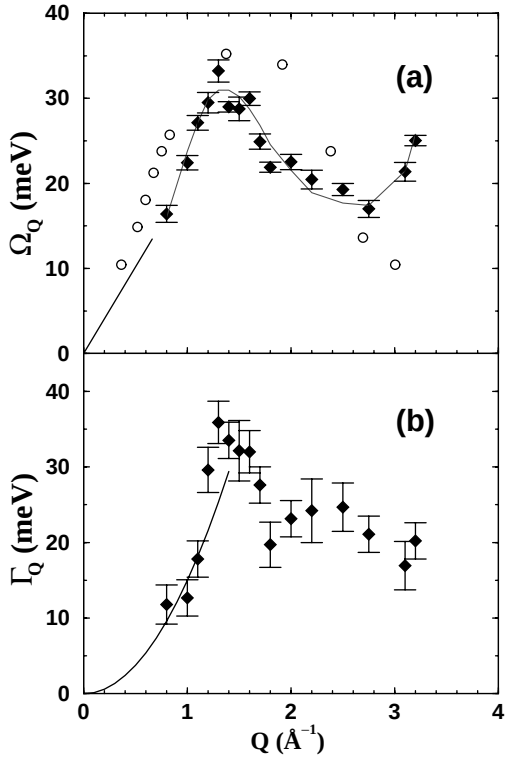

FIG. 2. Spectral parameters characterizing the collective excitation. (a) Excitation frequencies. The straight line represents hydrodynamic dispersion $\Omega_{\text{hyd}} = c_T Q$ with $c_T = 19.82$ meV Å. Experimental data are depicted by filled symbols. Open symbols stand for the simulation data of [10]. The line going through the data points is drawn as a guide to the eye. (b) Damping coefficient as given by the full width at half maximum of the inelastic peak. The line shows a fit to a hydrodynamic damping $\Gamma_{\text{hyd}} = D_{\text{hyd}} Q^2$ with $D_{\text{hyd}} = 15$ meV.

Such a relatively small reduction in frequencies suggests that what is being sampled in the melt can be thought of as remnants of crystal phonons. To see this, we make an estimate within the hydrodynamic realm of the amount of softening of the elastic constants upon melting. To proceed, we calculate a polycrystalline average of the crystal elasticity constant using published values of the constants including their temperature dependences [15]. If one then calculates the value for the melt from macroscopic sound velocity and density data [8], one arrives at a figure for the ratio of the liquid and crystal constants upon melting of 0.68, a respectable figure which shows that the strong binding forces of the crystal still are felt within the melt. The "dispersion curve" shown in Fig. 2a can thus be understood by reference to the orientationally averaged frequencies of the polycrystal.

From the ratios Ω_Q/Γ_Q it is inferred that the region of propagating density oscillations extends up to ≈ 1 Å^{-1}. The lifetimes estimated as Γ_Q^{-1} for the lowest accessible wave vector $Q = 0.8$ Å^{-1} give figures of ≈ 0.44 ps which translates into mean free paths (MFP) of about 13 Å. In consequence, one expects that the excitation MFP's will reach distances well beyond those characteristic of next-nearest neighbors at relatively large wave vectors (for $Q = 0.5$ Å^{-1} a lifetime of 1 ps and a MFP of 30 Å are expected.) A comparison of data for $Q = 0.8$ Å^{-1} with results from Ref. [10] shows that the simulation data overestimate the excitation frequencies by some 35% while predicting a linewidth which is in good agreement with the present result.

In a monatomic liquid the excitation lifetimes are shortened by viscous drag forces and heat flow effects which are additive up to first order and their relative weights can be estimated within the hydrodynamic limit [16] from values of thermodynamic quantities [17]. Here, viscous damping amounts to 6.3×10^1 Å^2 ps^{-1} while that related to heat conduction reaches 6.8×10^2 Å^2 ps^{-1}. The latter, which is much larger than those of the alkali metals, arises from the large thermal conductivity as well as from $(\gamma - 1)$ which is here 4 times larger than that of liquid Rb. The values just quoted, if extrapolated to $Q \approx 1$ Å^{-1}, would lead to damping coefficients much larger than the excitation frequencies, in stark contrast with experiment. Such an apparent paradox was solved some time ago by means of the introduction of a Q-dependent microscopic viscosity $\eta(Q)$ which approaches the hydrodynamic value as $Q \to 0$ but strongly decreases as Q increases. In our case, estimates of the linewidths for the Q values under consideration may be derived from $\eta(Q) = G(Q)\tau(Q)$ with $G(Q)$ given by Eqs. 8.81 of Ref. [3]. By taking values for the Einstein frequency $\omega_E = 4.2 \times 10^{13}$ s^{-1} and the relaxation time $\tau(Q)$ from the computer simulation work [10], one obtains a linewidth for $Q = 1$ Å^{-1} of ≈ 17 meV, not too far from the observed value. With regards to the heat-conduction term, fairly conclusive evidence from the analysis of computer simulations and experiments on dense rare-gas fluids [1] show that an even stronger Q dependence is to be expected for this term. In fact the very ratio of specific heats is believed to be Q dependent, reaching values close to unity at wave vectors somewhat below Q_p [18]. This therefore leaves the viscous term as the dominant contributor to damping. The latter can in turn be related to microscopic details by recourse to semiempirical treatments such as [19],

$$\eta_s = \frac{8\pi}{9}\,\omega_L M \rho_0^2 \int_0^a r^4 g(r)\,dr\,, \qquad (1)$$

with a denoting the first minimum of the $g(r)$ radial distribution. Equation (1) thus relates the damping to the Lindemann frequency ω_L [19], evaluated from thermodynamic properties at melting, a mass density term, and a contribution dependent upon the microscopic structure. The latter was evaluated from published data for the radial distributions [20] and yields 80.20 for Ni versus 539.7 for Na or 1561 for K. Such disparate values are partially compensated for by the mass density which makes the last two factors in Eq. (1) to be of the same order as that of Ni

(4 times larger than Na and ≈3 times that of K). Finally, the value of ω_L, which amounts to 15.5, 7.8, and 4.4 meV, respectively, serves to give a due account of the large differences in viscosity of liquid Ni and the molten alkali metals. In this respect it is worth remarking that while a large ω_L will increase the damping it will also increase the frequency of the excitation, and therefore the ratio η_s/ω_L is the quantity that matters concerning the character of the excitation (i.e., propagating or overdamped).

To explore whether the observed density oscillations result from specific details of the pair potential, we have considered that of Ni, alongside those of the molten alkali metals, as well as that of Ar in the same spirit as described in Ref. [6]. A criterion to quantify the extent that a liquid deviates from idealized behavior is given by $\gamma_G = -(r_0/6)\,(v'''(r)/v''(r))r_0$ where $v(r)$ is the pair potential, the primes stand for its derivatives, and r_0 is the location of its minimum. The quantity γ_G is thus interpreted as a Grüneisen parameter for next-neighbor interactions which vanishes for quadratic potentials. To proceed, use was made of the set of potential functions given in [20] (Na-Cs and Ni). The shapes of $v(r)$ about the main minimum were approximated by an anharmonic potential, including terms up to fifth order for the alkalis and to sixth order for Ni. The effective γ_G were then evaluated from the fitted functions, yielding figures for the heavier alkalis (Na-Cs) within 1.79–1.45 while that for Ni is ≈2.06. A 12-6 Lennard-Jones, known to accurately describe liquid Ar, has $\gamma_G = 3.5$ which is significantly larger than the rest. The figures just quoted thus show that it is the curvature of the main minimum of the potential that drives the dynamics of liquid Ni in a way much closer to that of the alkali metals than to liquid Ar. Other details, such as the softness of the repulsive cores or the radial extent covered by the ionic pair potential, seem to be of lesser importance.

In summary, the presence of well-defined excitations in a liquid with fairly anharmonic features in its thermodynamic functions shows that, contrary to current assumptions, the presence of *d* electrons or the absence of well defined Friedel oscillations in the pair potential does not rule out the ability of a liquid metal to sustain well-defined collective excitations. Moreover, these seem to be more dependent upon details of the microscopic interactions up to distances corresponding to nearest neighbors as quantified by γ_G than on the value of the thermodynamic γ. A quantitative understanding of the microscopic dynamics of transition metal liquids is needed to provide a way out of recent controversies concerning the viscosity of the earth's mantle for which estimates differing by many orders of magnitude are under discussion [9]. The mystery is all the more complete as studies on the elastic properties of one of the candidates to represent its composition (a Fe-Ni-S alloy) report large anomalies in their temperature and frequency dependences [9]. Studies of such alloys are now on the agenda, aiming to disentangle the microscopic mechanisms leading to these puzzling behaviors.

This work was supported in part by Grants No. PB98-0673-c02-01 and No. PB98-0536 from DGESIC (Spain).

[1] H. Bell, Phys. Rev. A **11**, 316 (1975); A. A. van Well *et al.*, Phys. Rev. A **31**, 3391 (1985).
[2] R. Eisenshitz and M. J. Wilford, Proc. Phys. Soc. London **80**, 1078 (1962).
[3] N. H. March, *Liquid Metals* (Cambridge University Press, Cambridge, UK, 1990).
[4] J. R. D. Copley and S. W. Lovesey, Rep. Prog. Phys. **38**, 461 (1975); R. L. McGreevy and E. W. J. Mitchell, Phys. Rev. Lett. **55**, 398 (1985).
[5] H. Sinn *et al.*, Phys. Rev. Lett. **78**, 1715 (1997); J. R. D. Copley and J. M. Rowe, Phys. Rev. Lett. **32**, 49 (1974); T. Bodensteiner *et al.*, Phys. Rev. A **45**, 5709 (1992); O. Söderstrom *et al.*, J. Phys. F **10**, L151 (1980).
[6] S. W. Lovesey, *Theory of Neutron Scattering from Condensed Matter* (Oxford Science Publications, Oxford, 1986), p. 214.
[7] F. J. Bermejo *et al.*, Phys. Rev. Lett. **84**, 5359 (2000); F. J. Bermejo *et al.*, Phys. Rev. B **60**, 15 154 (1999).
[8] T. Iida and R. I. L. Guthrie, *The Physical Properties of Liquid Metals* (Oxford Science Publications, Oxford, 1993), p. 170–187.
[9] P. M. Nasch *et al.*, Science **277**, 219 (1997); D. Alfe *et al.*, Phys. Rev. B **61**, 132 (2000).
[10] M. M. G. Alemany *et al.*, Phys. Rev. B **58**, 685 (1998).
[11] M. W. Johnson *et al.*, Phys. Chem. Liq. **6**, 243 (1977).
[12] B. C. Rambaut *et al.*, J. Phys. Condens. Matter **10**, 4221 (1998).
[13] H. R. Glyde, *Excitations in Liquid and Solid Helium* (Clarendon Press, Oxford, 1994), p. 187.
[14] R. J. Birgeneau *et al.*, Phys. Rev. **136**, 1359 (1964).
[15] G. Leibfried and W. Ludwig, in *Solid State Physics*, edited by F. Seitz and D. Turnbull (Academic Press, New York, 1961) Vol. 12, p. 366.
[16] Given by $\Gamma_{\text{hyd}} = \frac{1}{2}[\kappa(\gamma - 1)/\rho C_p + \nu]$, with ν being the longitudinal kinematic viscosity.
[17] See [8], Table 3.1, page 71, Table 4.3, page 91, and Table 6.3, page 183. See also H. Landolt-Bornstein, *Zahlenwerte und Funktionen aus Physik, Chemie, Astronomie, Geophysic und Technik* (Springer-Verlag, Berlin, 1964), 6th ed., Vol. IV, part 2b, p. 123. No data concerning bulk viscosities seem to be available.
[18] J. P. Boon and S. Yip, *Molecular Hydrodynamics* (McGraw-Hill, New York, 1980), p. 314.
[19] See Ref. [8], Chap. 6; and B. Djemili *et al.*, J. Less-Common Met. **79**, 29 (1981).
[20] J. L. Bretonnet and N. Jakse, Phys. Rev. B **50**, 2880 (1994); **43**, 8924 (1991).